

RESEARCH ARTICLE

WILEY

Development of pedotransfer functions for soil hydraulic properties in the critical zone on the Loess Plateau, China

Jiangbo Qiao¹  | Yuanjun Zhu² | Xiaoxu Jia³ | Laiming Huang³ | Ming'an Shao^{2,3}

¹College of Resources and Environment, Northwest A&F University, Yangling, China

²State Key Laboratory of Soil Erosion and Dryland Agriculture on the Loess Plateau, Northwest A&F University, Yangling, China

³Key Laboratory of Ecosystem Network Observation and Modeling, Institute of Geographic Sciences and Natural Resources Research, Chinese Academy of Sciences, Beijing, China

Correspondence

Yuanjun Zhu, State Key Laboratory of Soil Erosion and Dryland Agriculture on the Loess Plateau, Northwest A&F University, Yangling 712100, China.
Email: zhuyuanjun@foxmail.com

Funding information

Key Deployment Project of the Chinese Academy, Grant/Award Number: KFZD-SW-306; National Natural Science Foundation of China, Grant/Award Numbers: 41530854 and 41371242; international cooperation programme between China and England, Grant/Award Number: 41571130081

Abstract

Soil hydraulic properties (SHPs) including the soil water retention curve and saturated soil hydraulic conductivity (K_s) are crucial input data for simulations of soil water and solute transport in the Earth's critical zone. However, obtaining direct measurements of SHPs at a wide range of scales is time consuming and expensive. Pedotransfer functions (PTFs) are employed as an alternative method for indirectly estimating these parameters based on readily measured soil properties. However, PTFs for SHPs for the deep soil layer in the Earth's critical zone are lacking. In this study, we developed new PTFs in the deep soil profile for K_s and soil water retention curve on the Loess Plateau, China, which were fitted with the van Genuchten equation. In total, 206 data sets comprising the hydraulic and basic soil properties were obtained from three typical sites. Samples were collected from the top of the soil profile to the bedrock by soil core drilling. PTFs were developed between the SHPs and basic soil properties using stepwise multiple linear regression. The PTFs obtained the best predictions for K_s ($R_{adj}^2 = 0.561$) and the worst for van Genuchten α ($R_{adj}^2 = 0.474$). The bulk density and sand content were important input variables for predicting K_s , α , and θ_s , and bulk density, clay content, and soil organic carbon were important for n . The PTFs developed in this study performed better than existing PTFs. This study contains the first set of PTFs of SHPs to be developed for the deep profile on the Loess Plateau, and they may be applicable to other regions.

KEYWORDS

Earth's critical zone, Loess Plateau, pedotransfer functions, soil hydraulic properties

1 | INTRODUCTION

The Earth's critical zone (ECZ) is located from the top of the plant canopy vertically down to the weathered bedrock and is a key area for sustaining ecosystem function and human survival (Lin, 2010). The water cycle comprises the core process that links the cycling of materials in the ECZ. Hydrological models of soil water dynamics are effective tools for studying the water cycle in the ECZ. Soil hydraulic properties (SHPs), which include the soil water retention curve (SWRC) and saturated soil hydraulic conductivity (K_s), are important input parameters for hydrological models. However, obtaining direct measurements of SHPs is expensive, time consuming, and labour-intensive. Thus, an efficient pedotransfer function (PTF) is necessary

for producing reasonably accurate estimations of SHPs by using the basic soil properties as inputs and obtaining the hydraulic parameters as outputs (Bouma, 1989).

In recent decades, many PTFs have been developed for SHPs at different scales using various methods (Li, Chen, White, Zhu, & Zhang, 2007; Santra & Das, 2008; Schaap, Leij, & Genuchten, 2001; Wösten, Pachepsky, & Rawls, 2001; Yao et al., 2015). For example, Vereecken, Maes, Feyen, and Darius (1989) sampled the soil horizons in 40 important Belgian soil series and estimated the soil moisture retention characteristics based on the texture, bulk density (BD), and carbon content using multiple regression analysis. Wösten, Lilly, Nemes, and Bas (1999) developed PTFs for SHPs using a database of the hydraulic properties of European soils (HYPRES) by nonlinear regression

analysis. Schaap et al. (2001) presented a computer program (ROSETTA) based on neural network analyses for estimating the SWRC and Ks for soils in the United States. Li et al. (2007) used multiple linear regression analysis to estimate the SHPs of Fengqiu County soils on the North China Plain. Wang, Shao, and Liu (2012) predicted the SHPs for the Chinese Loess Plateau based on multiple linear regression equations, and Zhao, Shao, Jia, Nasir, and Zhang (2016) also used PTFs to estimate the soil hydraulic conductivity on the Loess Plateau of China by multiple linear regression and artificial neural networks. However, it should be noted that the previously developed PTFs for SHPs were mainly for upper soil layers (of depths <3 m), and no studies have considered the PTFs for deep layers in the ECZ.

The Loess Plateau area of China is predominantly covered by loessial deposits with thicknesses ranging from 50 to 200 m, and two thirds of this area contains arid and semi-arid regions. Thus, there is a need for reliable SHPs data to study the hydraulic processes that occur in the ECZ. However, it is difficult to obtain direct measurements of SHPs in deep soil profiles. Therefore, PTFs should be developed to obtain indirect estimates of the SHPs for deep soil profiles on the Loess Plateau.

Therefore, the objectives of the present study were (a) to characterize descriptive statistics for the SHPs of soil material at various depths on the Loess Plateau, (b) to develop PTFs for the SHPs in the ECZ on the Loess Plateau, and (c) to compare the results obtained using these new PTFs with those produced by existing PTFs.

2 | MATERIALS AND METHODS

2.1 | Study area description

The study was conducted across the entire Loess Plateau of China (33°43′–41°16′N, 100°54′–114°33′E), which is located in the continental monsoon climate region and covers approximately 6.5% of China (Figure 1a). The annual precipitation ranges from 150 mm in the northwest to 800 mm in the southeast, where 55–78% falls from June to September (Shi & Shao, 2000). The annual solar radiation ranges from 5.0×10^9 to 6.7×10^9 J m⁻². The annual evaporation on the Loess Plateau is 1,400–2,000 mm, and the mean annual temperature ranges from 3.6°C in the northwest to 14.3°C in the southeast (Shi & Shao, 2000). The region is surrounded by mountains, where the loessial landforms include Yuan (a large flat surface with little erosion), ridges, hills, and gullies.

2.2 | Soil sampling

Three typical sampling sites (Yangling, Changwu, and An'sai; Figure 1b) were selected from south to north on the Loess Plateau, and soil samples were collected from the soil surface to the bedrock using drilling equipment (assembled by Xi'an Qinyan Drilling Co. Ltd). At each sampling site, metal cylinders (diameter: 5 cm, length: 5 cm) were used to collect undisturbed soil samples from the midpoint of each 1-m interval of the soil boring (0.5, 1.5, 2.5, and 3.5 m ...) to obtain measurements of Ks, SWRC, and BD. Similarly, disturbed soil samples were collected to determine the soil particle composition and soil

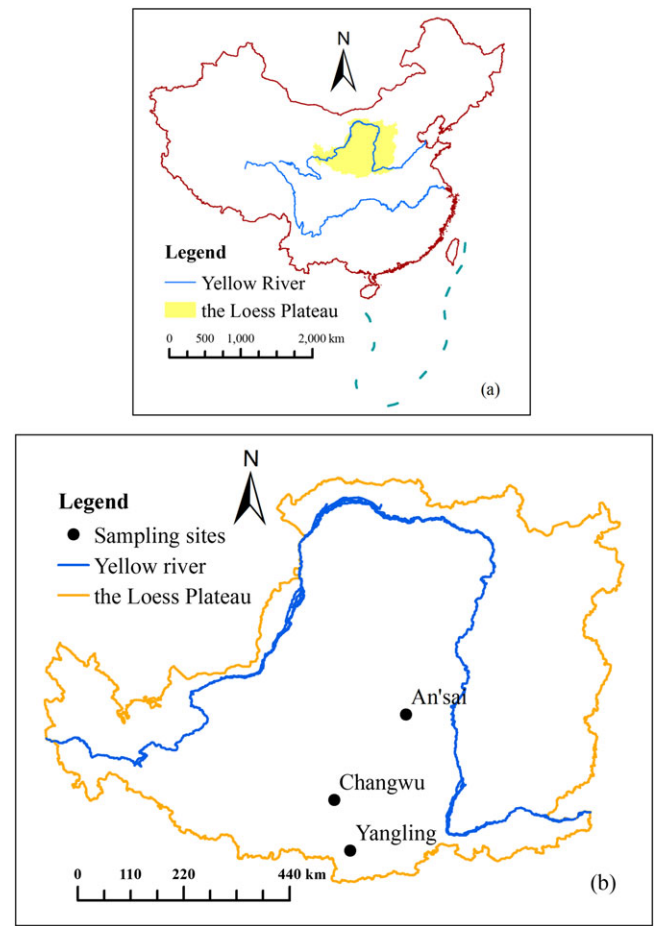


FIGURE 1 Location of the Loess Plateau region in China (a) and the sampling sites (b)

organic matter contents. It should be noted that the undisturbed soil samples were not replicated due to the possible cost incurred and challenges obtaining the samples. In addition, some soil cores were damaged during drilling. Therefore, the number of soil cores with SHPs that could be measured were 30, 100, and 76 for Yangling, Changwu, and An'sai, respectively. The corresponding soil drilling depths were 104.5, 204.5, and 161.6 m, respectively.

2.3 | Laboratory analysis

Ks was determined for undisturbed soil samples using the constant head method (Wang, Wang, Wei, Shao, & Li, 2008). The soil water retention data were measured by the centrifugation method (Hitachi CR21G centrifuge; 20°C) at suctions of 1, 10, 20, 40, 60, 80, 100, 200, 400, 600, 800, and 1,000 kPa (Lu, Shao, Horton, & Liu, 2004). The BD was determined based on the volume–mass relationship for each oven-dried core sample (105°C, 48 hr; Wang et al., 2008). The disturbed soil samples were also air-dried and passed through a 2.0-mm mesh before measuring the soil particle composition by laser diffraction (Mastersizer 2000, Malvern Instruments, Malvern, UK; Liu, Tong, & Li, 2005). The samples were also passed through a 0.25-mm mesh to determine the soil organic carbon (SOC) contents by dichromate oxidation (Nelson et al., 1982).

2.4 | Data analysis

2.4.1 | SWRC

The SWRC is influenced by many factors, including physical, chemical, and biological processes. Many models have been developed to fit the SWRC, such as the Gardner model (Gardner, Hillel, & Benyamini, 1970), Brooks–Corey model (Brooks & Corey, 1964), Mualem model (Mualem, 1976), van Genuchten (VG) model (Van Genuchten, 1980), and Campbell model (Campbell, 1974). The VG model is commonly used because it can be fitted to SHP data for a wide range of soil textures (Liu, Shu, & Wang, 2007). The equation for the VG model is

$$\theta(h) = \theta_r + \frac{(\theta_s - \theta_r)}{(1 + |ah|^n)^{1-\frac{1}{n}}}, \quad (1)$$

where $\theta(h)$ is the volumetric water content ($\text{cm}^3 \text{cm}^{-3}$) for the soil water pressure head h (cm), θ_s is the saturated soil water content ($\text{cm}^3 \text{cm}^{-3}$), θ_r is the residual soil water content ($\text{cm}^3 \text{cm}^{-3}$), α is a fitting parameter related to the inverse of the air entry pressure, and n is a fitting parameter related to the soil pore distribution.

2.4.2 | PTFs

In this study, the 206 soil samples were divided randomly into two groups: Group A (137) for deriving the PTFs (including calibration data sets for SHPs) and Group B (69) for validating the PTFs.

Many methods have been used to develop PTFs, such as multiple linear regression, nonlinear regression, and ANNs. Multiple linear regression is a traditional method for developing PTFs, where it is widely applicable, and it has been employed in soil science for developing the PTFs for soil parameters (Kai-Hua, Shao-Hui, Ji-Chun, Shu-Hua, & Qing, 2011; Li et al., 2007; Santra & Das, 2008; Wang et al., 2012). ANNs have also been applied successfully to the development of PTFs, and these generally perform better than other PTFs (Vereecken et al., 2010; Yao et al., 2015). However, large data sets are needed to obtain good estimates using ANNs (Agyare, Park, & Vlek, 2007; Patil, Rajput, Singh, & Singh, 2009). Therefore, in the present study, stepwise multiple linear regression was performed to select the most significant input variables, before investigating the ln-transformed, reciprocal, quadratic, and square root transformations of the variables. The equation for regression analysis is as follows:

$$Y = \alpha_0 + \alpha_1 X_1 + \alpha_2 X_2 + \dots + \alpha_5 X_5 + \alpha_6 X_1^{-1} + \dots + \alpha_{10} X_2^{-1} + \alpha_{11} X_1^2 + \dots + \alpha_{15} X_5^2 + \alpha_{16} \ln X_1 + \dots + \alpha_{20} \ln X_5 + \alpha_{21} e^{X_1} + \dots + \alpha_{25} e^{X_5}, \quad (2)$$

where Y is the dependent variable (K_s , α , n , or θ_s), α_0 is the intercept, $\alpha_1, \dots, \alpha_{25}$ are regression coefficients, and X_1 – X_5 are the independent variables (BD, sand, silt, clay, and SOC).

The predictive capacities of the new PTFs were evaluated based on the adjusted R^2 value calculated by

$$R_{adj}^2 = 1 - (1 - R^2) \left[\frac{N-1}{N-M-1} \right], \quad (3)$$

where N is the number of observations, M is the number of independent variables in the PTF, and R^2 is the coefficient of determination.

In addition, the performance of the new PTFs was determined based on three indexes, the coefficient of determination (R^2), the root mean squared error (RMSE), and the mean error (ME), defined as follows:

$$R^2 = 1 - \frac{\sum_{i=1}^N (y_i - \hat{y}_i)^2}{\sum_{i=1}^N (y_i - \bar{y})^2}, \quad (4)$$

$$RMSE = \sqrt{\frac{\sum_{i=1}^N (y_i - \hat{y}_i)^2}{N}}, \quad (5)$$

$$ME = \frac{\sum_{i=1}^N (y_i - \hat{y}_i)}{N}, \quad (6)$$

where y_i is the measured value, \hat{y}_i is the predicted value, \bar{y} is the mean of the measured value, and N is the number in Group A.

2.5 | Statistical analysis

The data were analysed with different software packages. Descriptive statistical analyses (including a calculation of the maximum, minimum, average, and coefficient of variation [CV]), Pearson's correlation analysis, and linear regression analysis were performed with SPSS (version 16.0). Nonlinear regression was conducted for the SWRCs using RETC software (version 6.0).

3 | RESULTS

3.1 | Statistical characteristics of SHPs

We used the VG equation to fit the SWRC soil data (corresponding to the water contents at suctions of 1, 10, 20, 40, 60, 80, 100, 200, 400, 600, 800, and 1,000 kPa). The results showed that the coefficients of determination (R^2) all exceeded 0.98. Therefore, the soil samples fitted the VG equation well. Table 1 shows the descriptive statistics for the VG parameters and K_s at all of the sampling sites. The mean values of K_s and α ranged from 0.002 to 0.007 cm min^{-1} and from 0.002 to 0.005 cm^{-1} , respectively. The mean values of n and θ_s ranged from 1.192 to 1.283 and from 0.420 to 0.439 $\text{cm}^3 \text{cm}^{-3}$, respectively. The SHPs differed significantly among the sampling sites ($P < 0.01$). The CV is an indicator of the overall variation of a given variable. At all of the sampling sites, there was high variation in K_s ($\text{CV} \geq 100\%$), moderate variation in α ($10\% < \text{CV} < 100\%$), and low variation in n (except at An'sai) and θ_s ($\text{CV} \leq 10\%$; Table 1; Nielsen & Bouma, 1985). Thus, the variations in SWRC in the deep soil profile were small compared with those in K_s on the Loess Plateau.

3.2 | Correlation analysis

Before developing the new PTFs, we investigated the possible relationship between the SHPs and soil properties. Table 3 shows the Pearson's correlation coefficients that were calculated among the variables based on the calibration data sets (Table 2). The results show that there were significant and positive correlations among the SHPs ($P < 0.01$). For example, K_s had significant positive correlations with α ,

TABLE 1 Descriptive statistics of the soil hydraulic properties for the sampling sites

	Variables	No.	Min	Max	Mean	SD	CV	K	S
Yangling	K_s (cm min ⁻¹)	30	1.0*10 ⁻⁴	0.058	0.007	0.012	1.730	2.941	10.152
	α (cm ⁻¹)	30	0.001	0.010	0.004	0.002	0.577	1.004	-0.101
	n	30	1.083	1.493	1.192	0.070	0.058	2.716	12.098
	θ_s (cm ³ cm ⁻³)	30	0.370	0.490	0.439	0.027	0.061	-0.496	0.596
Changwu	K_s (cm min ⁻¹)	101	1.3*10 ⁻⁶	0.040	0.002	0.005	2.746	4.717	26.609
	α (cm ⁻¹)	101	0.0004	0.008	0.002	0.001	0.590	1.466	2.396
	n	101	1.138	1.974	1.301	0.123	0.095	3.365	14.884
	θ_s (cm ³ cm ⁻³)	101	0.378	0.472	0.420	0.023	0.056	0.170	-0.744
An'sai	K_s (cm min ⁻¹)	76	2.8*10 ⁻⁵	0.036	0.006	0.007	1.340	2.106	4.479
	α (cm ⁻¹)	76	0.001	0.011	0.005	0.002	0.405	0.118	-0.654
	n	76	1.122	1.985	1.382	0.232	0.168	0.984	-0.064
	θ_s (cm ³ cm ⁻³)	76	0.350	0.508	0.428	0.031	0.073	-0.330	-0.164

Note. No.: number; Min: minimum; Max: maximum; SD: standard deviation; CV: coefficient of variation; K: Kurtosis; S: Skewness.

TABLE 2 Descriptive statistics of the soil hydraulic properties in the calibration data and the evaluation parameters of the output from the developed pedotransfer functions

Variables	No.	Min	Max	Mean	S.D.	CV	R ²	RMSE	ME
K_s (cm min ⁻¹)	138	1.3*10 ⁻⁶	0.058	0.004	0.009	1.926	0.566	0.006	0.00004
α (cm ⁻¹)	138	0.00056	0.011	0.004	0.002	0.632	0.481	0.002	0.001
n	138	1.083	1.985	1.321	0.184	0.139	0.532	0.126	0.008
θ_s (cm ³ cm ⁻³)	138	0.350	0.490	0.426	0.027	0.064	0.513	0.019	0.0005

Note. No: number; Min: minimum; Max: maximum; SD: standard deviation; CV: coefficient of variation; R²: coefficient of determination; RMSE: root mean square error; ME: mean error.

n , and θ_s . In addition, K_s had significant correlations with all of the selected variables except for SOC ($P < 0.01$), which indicates that SOC was not an important factor for K_s . The α and n parameters had significant correlations with all of the selected variables ($P < 0.01$). There were significant correlations between θ_s and BD, sand, and clay, and there were also high correlations with BD and clay ($P < 0.01$), but there were no correlations with silt and SOC. The results obtained by correlation analysis were used to develop the new PTFs for SHPs (Table 3).

3.3 | New PTFs for SHPs

Stepwise multiple regression analysis was performed to develop new PTFs for the SHPs by using the basic soil properties that had significant

correlations with the SHPs, including their different forms (reciprocal, quadratic, etc.). Table 4 shows the regression equations and the adjusted R² values for the new PTFs. Analysis of variance showed that all of the new PTFs were highly significant ($P < 0.001$), where most of the standardized residuals from the regression were distributed randomly between -2 and +2. Thus, there were no significant correlations between the standardized residuals and the standardized predicted values. Therefore, the new PTFs satisfied the assumption of linearity with no statistical bias, and they could provide robust predictions of the SHPs.

The adjusted R² values determined for the new PTFs for SHPs ranged from 47.4% to 56.1%, thereby indicating that their predictive capacities differed. The best model was obtained for K_s , which explained 56.1% of the total variation, whereas the worst was for α ,

TABLE 3 Pearson correlation analysis between soil hydraulic properties and soil properties

Variables	K_s	α	n	θ_s	BD	Sand	Silt	Clay	SOC
K_s	1	0.42**	0.37**	0.33**	-0.54**	0.33**	-0.26**	-0.27**	0.140
α	0.42**	1	0.42**	0.42**	-0.23**	0.65**	-0.42**	-0.59**	-0.27**
n	0.37**	0.42**	1	0.26**	-0.25**	0.62**	-0.33**	-0.61**	-0.28**
θ_s	0.33**	0.42**	0.26**	1	-0.61**	0.21*	-0.04	-0.25**	-0.04
BD	-0.54**	-0.23**	-0.25**	-0.61**	1	0.04	-0.04	-0.02	-0.31**
Sand	0.33**	0.65**	0.62**	0.21*	0.030	1	-0.70**	-0.88**	-0.43**
Silt	-0.26**	-0.42**	-0.33**	-0.040	-0.04	-0.70**	1	0.26**	0.30**
Clay	-0.27**	-0.59**	-0.61**	-0.25**	-0.02	-0.88**	0.26**	1	0.37**
SOC	0.14	-0.27**	-0.28**	-0.040	-0.31**	-0.43**	0.30**	0.37**	1

Note. BD: bulk density; SOC: soil organic carbon.

* Correlation significant at $P < 0.05$ (two-tailed).

**Correlation significant at $P < 0.01$ (two-tailed).

TABLE 4 Pedotransfer functions developed for soil hydraulic properties

Model parameters	Regression equations	Adjusted R^2
K_s	$-1.523 + 1.685*BD^{-1} + 0.0004*Sand + 0.996*lnBD$	0.561
α	$0.012 + 0.0002*Sand - 0.007*BD$	0.474
n	$5.507 + 6.966*Clay^{-1} - 7.272*BD^2 + 0.186*SOC^{-1} - 4.399*BD^{-1}$	0.526
θ_s	$-0.779 - 0.608*BD^2 + 0.016*lnSand + 1.712*BD - 0.000027*Sand^2$	0.519

which explained 47.4% of the total variation. It is interesting that the capacity for predicting K_s was the highest because it is usually considered to have low R^2 values with most PTFs (Wang et al., 2012; Wösten et al., 1999). Although the PTFs developed in previous studies were for predicting K_s only in the upper soil layers of different regions, it is possible that K_s is influenced by only a few factors in the deep soil layers (e.g., soil texture, BD, and SOC), whereas it may be influenced by many factors in the upper layer (e.g., soil texture, vegetation coverage, and human activities). Therefore, our PTFs obtained higher R^2 values for the predictions of K_s .

In addition, the stepwise multiple regression analysis identified factors that had significant correlations with the SHPs. Among all of the SHPs (except for n), BD and sand were important input variables for the regression equations. Thus, BD and sand were important factors for predicting the SHPs in the deep profiles. In addition, BD, clay, and SOC were important input variables for predicting n .

The accuracy of the new PTFs was evaluated using the calibration data, and Table 2 shows the values obtained in terms of R^2 , the RMSE, and ME. The values of R^2 and RMSE ranged from 0.481 to 0.566 and from 0.002 to 0.126, respectively, thereby indicating that the accuracies of the predictions differed among the new PTFs. The ME values were all greater than zero, thereby indicating that the SHPs were underestimated by the new PTFs. In addition, the performance of developed PTF models was tested by using the validation data sets (Table 6). The values of R^2 and RMSE ranged from 0.375 to 0.625 and from 0.002 to 0.144, respectively, which were similar to that attained by the calibration data sets.

3.4 | Comparison with existing PTFs

We compared the performance of three existing PTFs (Table 5) and the new PTFs based on the validation data, and the evaluation indexes obtained for the PTFs are shown in Table 6. Figure 2 also compares the performance of the new and existing PTFs by predicting all of the SHPs as scatter plots (except for K_s). Compared with the other

TABLE 6 Values of the evaluation indicators obtained for the new and existing pedotransfer functions (PTFs) using the validation data

Evaluation indicator	PTFs	K_s	θ_s	α	n
R^2	This study	0.625	0.378	0.277	0.350
	Li	0.008	0.170	0.004	0.176
	HYPRES	0.646	0.262	0.095	0.261
	Wang		0.106		
RMSE	This study	0.005	0.023	0.002	0.144
	Li	1776.144	0.091	0.004	0.187
	HYPRES	170.054	0.042	0.066	0.549
	Wang		0.071		
ME	This study	-0.001	0.002	0.001	-0.014
	Li	-435.573	0.072	0.002	0.044
	HYPRES	-158.689	-0.006	-0.066	-0.530
	Wang		-0.002		

Note. R^2 : coefficient of determination, RMSE: root mean square error; ME: mean error.

PTFs, the new PTFs had higher R^2 values, whereas the values of RMSE and ME were lower, thereby indicating the improved performance of the new PTFs in the study area. Clearly, there were obvious limitations when applying the PTFs developed for other regions, as shown in other studies (Li et al., 2007; Wang et al., 2012).

We also found that the RMSE and ME values obtained by the other PTFs for K_s were greater than 100 and even up to 1,000, possibly because K_s was much lower in the deep soil layer than the upper soil layer, thereby obtaining poor predictions with the three existing PTFs.

In addition, in terms of the capacity to predict the SHPs of new PTFs and existing PTFs (Table 5), the HYPRES PTFs, which were developed for Europe, ranked second best, and the Li PTFs, which were developed for other regions in China, ranked third best. The databases used for developing the PTFs in the aforementioned studies were different. The PTFs developed by Li comprised data for 63 SWRCs and 36 saturated soil hydraulic conductivities, whereas more than 5,000 were used in the HYPRES PTFs. Therefore, the predictive capacity of the HYPRES PTFs was better compared with that of the PTFs developed by Li.

In this study, we obtained important data for SHPs to study the hydraulic processes and hydrologic models in the ECZ. In addition, we developed the first PTFs for soil SHPs in deep soil layers, and they performed better than existing PTFs. These new PTFs could save time, labour, and money and improve the efficiency of research of the ECZ in the study area.

TABLE 5 Established pedotransfer functions (PTFs) used for comparison with new PTFs developed in this study

PTFs	Source database	Methodology to develop PTFs	Hydraulic parameter	Input variables	Country
Li et al. (2007)	Fengqiu County ($N = 63$ and 36)	Multiple linear regression	K_s, α, n, θ_s	BD, SOC, silt, clay, sand	China
HYPRES (Wösten et al., 1999)	HYPRES database ($N = 5,521$)	Nonlinear regression	K_s, α, n, θ_s	BD, SOC, silt, clay, horizon	Europe
Wang et al. (2012)	The Loess Plateau ($N = 252$)	Multiple linear regression	K_s, FC, θ_s	BD, SOC, sand, silt, clay, altitude	China

Note. BD: bulk density; SOC: soil organic carbon; FC: field capacity.

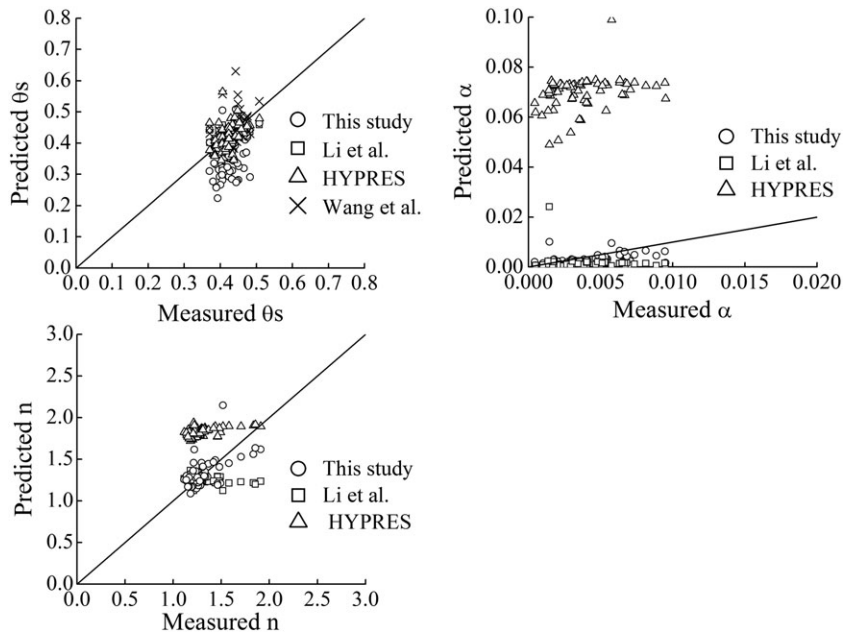


FIGURE 2 Measured and predicted values of soil hydraulic properties by the new pedotransfer function (PTF) and other established PTFs in validation data sets. The established PTFs are Li et al. (2007), HYPRES (Wösten et al., 1999) and Wang et al. (2012). The straight line in each plot is the 1:1 line

4 | DISCUSSION

The Loess Plateau area of China is predominantly covered by deep loessial deposits (generally 50–200 m), which are subject to intense soil erosion. However, it is difficult to obtain direct measurements of SHPs for the deep soil layer (generally 50- to 200-m depth) on the Loess Plateau, thereby making it necessary to employ related PTFs. Until now, PTFs were not available for the SHPs of the deep soil layer on the Loess Plateau. Wang et al. (2012) also developed PTFs for the SHPs on the Loess Plateau, China, but they focused mainly on the upper layer (0–5 cm), which is not sufficiently deep for the Loess Plateau. In addition, the SHPs of the deep soil layer differ from those in the upper layer, especially for K_s .

Therefore, we developed the first set of PTFs for the SHPs of the deep layers on the Loess Plateau, China, thereby improving the efficiency of research into the water cycle (such as water movement in the thick unsaturated zone and the pattern of precipitation supplying groundwater) and facilitating the development of relevant hydrological models of the Loess Plateau. This study may contain the first set of PTFs developed for very deep soil layers anywhere in the world, and they may be applicable to deep soil layers in other regions. A limitation of our study was that the number of soil samples was small, which was due to the difficulty of obtaining samples from such deep soil layers. Further research is necessary to obtain more undisturbed soil samples from deep soil layers.

5 | CONCLUSION

In this study, we measured SHPs and basic soil properties at three typical sites (Yangling, Changwu, and An'sai) on the Loess Plateau, China. Samples were collected from the top of the soil profile to the bedrock by soil core drilling. We used the results to develop new PTFs by stepwise multiple linear regression. The results showed that at all of the sampling sites, there was high variation in K_s , moderate

variation in α and n (except at An'sai), and low variation in θ_s . The adjusted R^2 values obtained for the new PTFs for SHPs ranged from 47.4% to 56.1%. The PTFs performed best for K_s ($R_{adj}^2 = 0.561$) and worst for α ($R_{adj}^2 = 0.474$). BD and sand were the most important input variables for predicting K_s , α , and θ_s , whereas BD, clay, and SOC were the most important for n . The PTFs developed in this study performed better when compared with existing PTFs. In this study, we obtained important data for SHPs to facilitate the study of hydraulic processes, and we developed the first PTFs for SHPs in deep soil profiles in the ECZ.

ACKNOWLEDGMENTS

This study was supported by the National Natural Science Foundation of China for a major international cooperation programme between China and England (41571130081), the National Natural Science Foundation of China (41371242 and 41530854), and the Key Deployment Project of the Chinese Academy (KFZD-SW-306). The authors thank the editor and reviewers for their valuable comments and suggestions.

ORCID

Jiangbo Qiao  <http://orcid.org/0000-0002-9448-6157>

REFERENCES

- Agyare, W. A., Park, S. J., & Vlek, P. L. G. (2007). Artificial neural network estimation of saturated hydraulic conductivity. *Vadose Zone Journal*, 6, 423.
- Bouma, J. (1989). Using soil survey data for quantitative land evaluation. *Advances in Soil Sciences*, 9, 177–213.
- Brooks, R. H., & Corey, A. T. (1964). Hydraulic properties of porous media and their relation to drainage design. *Transactions of the ASAE*, 7, 26–0028.
- Campbell, G. S. (1974). A simple method for determining unsaturated conductivity from moisture retention data. *Soil Science*, 117, 311–314.
- Gardner, W., Hillel, D., & Benyamini, Y. (1970). Post-irrigation movement of soil water: 1. Redistribution. *Water Resources Research*, 6, 851–861.

- Kai-Hua, L., Shao-Hui, X., Ji-Chun, W., Shu-Hua, J., & Qing, L. (2011). Assessing soil water retention characteristics and their spatial variability using pedotransfer functions. *Pedosphere*, 21, 413–422.
- Li, Y., Chen, D., White, R. E., Zhu, A., & Zhang, J. (2007). Estimating soil hydraulic properties of Fengqiu County soils in the North China Plain using pedo-transfer functions. *Geoderma*, 138, 261–271.
- Lin, H. (2010). Earth's critical zone and hydrogeology: Concepts, characteristics, and advances. *Hydrology & Earth System Sciences*, 6, 3417–3481.
- Liu, Y. P., Tong, J., & Li, X. N. (2005). Analysing the silt particles with the Malvern Mastersizer 2000. *Water Conservancy Science & Technology & Economy*, 11(6), 329–331.
- Liu, Z., Shu, Q., & Wang, Z. (2007). Applying pedo-transfer functions to simulate spatial heterogeneity of Cinnamon soil water retention characteristics in Western Liaoning Province. *Water Resources Management*, 21, 1751–1762.
- Liu, D., Shao, M., Horton, R., & Liu, C. (2004). Effect of changing bulk density during water desorption measurement on soil hydraulic properties. *Soil Science*, 169, 319–329.
- Mualem, Y. (1976). A new model for predicting the hydraulic conductivity of unsaturated porous media. *Water Resources Research*, 12, 513–522.
- Nelson, D. W., Sommers, L. E., Sparks, D. L., Page, A. L., Helmke, P. A., Loeppert, R. H., et al. (1982). Total carbon, organic carbon, and organic matter. *Methods of Soil Analysis Part—Chemical Methods*, 961–1010.
- Nielsen, D. R., & Bouma, J. (1985). Soil spatial variability: proceedings of a workshop of the ISSS and the SSSA, Las Vegas, USA, 30 November - 1 December, 1984Pudoc.
- Patil, N. G., Rajput, G. S., Singh, R. B., & Singh, S. R. (2009). Development and evaluation of pedotransfer functions for saturated hydraulic conductivity of seasonally impounded clay soils. *Agropedology*, 47–56.
- Santra, P., & Das, B. S. (2008). Pedotransfer functions for soil hydraulic properties developed from a hilly watershed of Eastern India. *Geoderma*, 146, 439–448.
- Schaap, M. G., Leij, F. J., & Genuchten, M. T. V. (2001). Rosetta: A computer program for estimating soil hydraulic parameters with hierarchical pedotransfer functions. *Journal of Hydrology*, 251, 163–176.
- Shi, H., & Shao, M. (2000). Soil and water loss from the Loess Plateau in China. *Journal of Arid Environments*, 45, 9–20.
- Van Genuchten, M. T. (1980). A closed-form equation for predicting the hydraulic conductivity of unsaturated soils. *Soil Science Society of America Journal*, 44, 892–898.
- Vereecken, H., Weynants, M., Javaux, M., Pachepsky, Y., Schaap, M. G., & Genuchten, M. T. V. (2010). Using pedotransfer functions to estimate the van Genuchten-Mualem soil hydraulic properties: A review. *Vadose Zone Journal*, 9, 795–820.
- Vereecken, H. J., Maes, J., Feyen, J., & Darius, P. (1989). Estimating the soil moisture retention characteristic from texture, bulk density, and carbon content. *Soil Science*, 148, 389–403.
- Wang, L., Wang, Q., Wei, S., Shao, M. A., & Li, Y. (2008). Soil desiccation for Loess soils on natural and regrown areas. *Forest Ecology & Management*, 255, 2467–2477.
- Wang, Y., Shao, M. A., & Liu, Z. (2012). Pedotransfer functions for predicting soil hydraulic properties of the Chinese Loess Plateau. *Soil Science*, 177, 424–432.
- Wösten, J. H. M., Lilly, A., Nemes, A., & Bas, C. L. (1999). Development and use of a database of hydraulic properties of European soils. *Geoderma*, 90, 169–185.
- Wösten, J. H. M., Pachepsky, Y. A., & Rawls, W. J. (2001). Pedotransfer functions: Bridging the gap between available basic soil data and missing soil hydraulic characteristics. *Journal of Hydrology*, 251, 123–150.
- Yao, R. J., Yang, J. S., Wu, D. H., Li, F. R., Gao, P., & Wang, X. P. (2015). Evaluation of pedotransfer functions for estimating saturated hydraulic conductivity in coastal salt-affected mud farmland. *Journal of Soils and Sediments*, 15, 902–916.
- Zhao, C., Shao, M. A., Jia, X., Nasir, M., & Zhang, C. (2016). Using pedotransfer functions to estimate soil hydraulic conductivity in the Loess Plateau of China. *Catena*, 143, 1–6.

How to cite this article: Qiao J, Zhu Y, Jia X, Huang L, Shao M. Development of pedotransfer functions for soil hydraulic properties in the critical zone on the Loess Plateau, China. *Hydrological Processes*. 2018;32:2915–2921. <https://doi.org/10.1002/hyp.13216>